Technical University of Denmark

DTU

Wetting controlled phase transitions in two-dimensional systems of colloids

Gil, Tamir; Ipsen, John Hjorth; Tejero, T.F.

Link back to DTU Orbit

DTU Library
Technical Information Center of Denmark

Wetting controlled phase transitions in two-dimensional systems of colloids

Tamir Gil and John Hjort Ipsen

Department of Chemistry, Technical University of Denmark, DK-2800 Lyngby, Denmark

Carlos F. Tejero

Facultad de Ciencias Físicas, Universidad Complutense de Madrid, 28040 Madrid, Spain

(Received 29 September 1997)

The phase behavior of disk colloids, embedded in a two-dimensional fluid matrix that undergoes a first-order phase transition, is studied in the complete wetting regime where the thermodynamically metastable fluid phase is stabilized at the surface of the disks. In dilute collections of disks, the tendency to minimize the extent of the fluid-fluid interface and the extent of the unfavorable wetting phase in the system gives rise to aggregation phenomena and to separation of large domains of disks that have the characteristics of bulk colloidal phases. The conditions for phase transitions among cluster gas, liquid, and solid phases of the disk colloids are determined from the corresponding values of the disk chemical potential within an analytic representation of the grand partition function for the excess energy associated with a gas of disk clusters in the low-disk-density limit. The wetting effective-interface potential is combined with the disk interaction potential in associating an internal energy with each one of the clusters. The theory can thus be applied to any type of interaction potential among disks, provided that the free energy associated with the corresponding bulk colloidal phases is available. A phase diagram is calculated explicitly for the case of hard disks on the basis of an analytical approximation for the free energy of the hard disk fluid phase and the generalized effective liquid approximation for the free energy of the hard disk solid phase. [S1063-651X(98)00203-7]

PACS number(s): 68.45.Gd, 64.70.−p, 82.70.Dd

I. INTRODUCTION

In general, when two thermodynamic phases α and β are close to coexistence, i.e., close to a first-order phase transition line, the presence of a substrate strongly "preferring" one of the phases leads to singular *wetting* effects [1]. The preferred phase β tends to form a layer intruding between the substrate and the other phase α, even when the latter is stable in the bulk. In the *complete wetting* regime, the thickness l_W of the layer diverges continuously, $l_W \rightarrow \infty$, as the bulk $\alpha \rightarrow \beta$ phase transition line is approached (Fig. 1).

Wetting of silica spheres by fluid lutidine (β) in a water solution (α), close to the fluid water-lutidine coexistence conditions, was first suggested as the cause for their reversible aggregation, called *flocculation*, in the celebrated paper by Beysens and Esteve [2]. Subsequently, particle aggregation phenomena have been reported in several other phase-separating binary mixtures [3]. Recently, based on computer calculations on a pseudo-two-dimensional microscopic model of lipid-protein interaction, wetting was suggested as a means of protein organization in membranes [4]. These are particular examples within the general interest in how the phases exhibited by systems of colloids are manipulated by controlling the properties of their embedding environment. Concordantly, in this study we consider an α-embedded two-dimensional dilute system of β-wet disk colloids in the complete wetting regime, close to the α-β first-order transition line. The tendency to minimize the extent of the α-β fluid-fluid interface and the extent of the unfavorable β phase in the system gives rise to aggregation phenomena that reflect the balance between those tendencies, and the tendency to increase entropy by separating the disks from each other. This balance changes as the α-β first-order transition line is

approached. Consequently, one can expect a transition from an α-embedded cluster gas of disks to a β-rich phase of disks, which has the characteristics of a bulk phase of disk colloids.

From the theoretical side, wetting-induced flocculation phenomena have been studied by applying a Ginzburg-Landau model to describe the embedding fluid matrix by a one-component order parameter, which is coupled to the co-
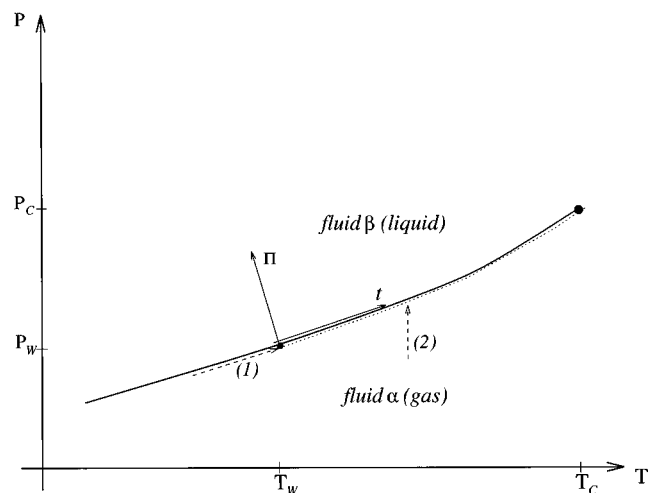
FIG. 1. The generic phase diagram for wetting by one of two fluid phases (β) at the bulk coexistence line with the other (α), shown by a thick solid line. *Critical wetting* transition occurs at T_W by increasing the temperature along the α-β coexistence curve, as shown by path (1). For $T > T_W$, any path taken in the direction of the arrow (2) would terminate in a continuous *complete wetting* as the α-β coexistence curve is approached.

ordinates that represent the location of sphere colloids [5]. Based on this model, simple thermodynamic considerations have led to a qualitative phase diagram, including regions of α-embedded spheres, β-embedded spheres, and the coexistence of the two phases. Computer calculations on the model have led to more precise topologies of the different phases, but consumed more computation time than to allow the production of a full phase diagram.

In this study we exploit the simplicity involved in the effective interface potential description of the wetting phenomenology (Secs. II and IV). Its application within a straightforward and exactly solvable way of writing the grand partition function for the excess energy associated with a gas of disk clusters in the low-disk-density limit (Sec. III) is the basis for a theory that enables the calculation of the conditions at which flocculation occurs. More specifically, we relate the value of the disk chemical potential at the transition between α-embedded disk cluster gas and β-embedded disk systems to the chosen thermodynamic control parameters (Sec. V). The entropy associated with the spatial organization of the disks plays a crucial role in the description of our system, and the total number of phases the system exhibits depends on the number of colloidal phases the disks exhibit in the bulk. In Sec. VI we calculate quantitatively the phase diagram that separates among regions of α-embedded hard disk cluster-gas and β-embedded hard disk systems, and the corresponding coexistence regions. Within the equilibrium regions of β-embedded hard disk systems, we distinguish between fluid and solid hard-disk colloidal phases, assuming this transition to be first order. We describe the fluid hard disk phase by an approximate analytical form for the free energy, which provides the best combination between simplicity and agreement with results obtained by numerical simulations [6]. For the solid phase we apply the differential formulation of the generalized effective liquid approximation (GELA) [7] with an approximate analytical expression for the direct correlation function of hard disks within the Percus-Yevick equation [8]. We start our discussion by introducing the effective interface potential in the description of wetting in circular geometry.

II. WETTING IN CIRCULAR GEOMETRY–
A RECOLLECTION

In planar geometry, a scaling description of the mean thickness of the wetting layer is achieved in terms of two orthogonal fields: one pressurelike field Π measures the difference in the grand canonical potentials per unit volume (or, area in two-dimensional geometry) of the two bulk phases; the other, temperaturelike field t is a generalized coordinate measuring the distance from the wetting transition point (P_W, T_W) along the coexistence line shown in Fig. 1. In terms of these fields, the continuous growth of the wetting layer is characterized by the power laws $l_W \propto \Pi^{-\Psi^c}$, $\Pi \to 0^+$, in the complete wetting regime, and $l_W \propto t^{-\Psi}$, $t \to 0^+$, along the coexistence line. The comprehensive description is achieved with a scaling function $\Phi(x)$ and a two-parameter scaling form

$$l_W \sim t^{-\Psi} \Phi[\Pi/t^\Delta], \quad \Phi(x) = \begin{cases} \text{const}, & x \to 0 \\ x^{-\Psi^c}, & x \to +\infty, \end{cases} \quad (1)$$

where $\Delta \equiv \Psi/\Psi^c$. The values of the exponents Ψ^c and Ψ depend on the spatial dimension of the system under consideration [1].

Increasing the thickness of a wetting layer around a spherical, or a cylindrical (circular), substrate leads to an increase in the area (length) of the interface. The corresponding increase in the interfacial free energy suppresses complete wetting at $\Pi = 0$. Hence the divergence of the mean thickness of the wetting layer can only occur in the limit where the curvature of the substrate vanishes, adding this curvature as a third field in the scaling description. In two dimensions, the mean thickness of the wetting layer around a circular disk of radius r_0 was shown to obey the scaling form [9]

$$l_W = \sigma^{-1/3} r_0^{1/3} Y(\Pi r_0/\sigma), \quad Y(x) \sim \begin{cases} \text{const}, & x = 0 \\ x^{-1/3}, & x \to \infty, \end{cases} \quad (2)$$

where σ is the *stiffness* of the α-β interface. σ defines a length scale in the system that we shall call the *bulk correlation length*,

$$\xi_b \equiv k_B T/\sigma, \quad (3)$$

where k_B is the Boltzmann constant and T is the temperature [10]. From Eqs. (2) and (3), the *complete wetting regime*, i.e., the conditions for the emergence of a macroscopic wetting layer of thickness $\sim r_0^{1/3}$ much larger than the molecular distances $\sim \xi_b$, is defined as [11]

$$r_0 \gg \xi_b, \quad T_W < T < T_C, \quad \sigma/r_0 \gg \Pi \to 0^+, \quad (4)$$

where T_C is the bulk α-β critical point and T_W is the wetting temperature for the analogous flat system.

The replacement of the density profile of the fluid-fluid (α-β) interface by a sharp kink, to which a local interfacial stiffness (σ) is attached, is valid in the complete wetting regime [1], where the wetting of a disk is properly described by an *effective interface grand canonical potential* [9,11]

$$\Omega(l_W) = 2\pi V(l_W) + 2\pi\sigma(r_0 + l_W) + \pi\Pi[(r_0 + l_W)^2 - r_0^2], \quad (5)$$

where $V(R) \equiv 0.948 r_0 (k_B T)^2/(\sigma R^2)$. The term $\pi\Pi[(r_0 + l_W)^2 - r_0^2]$ in this equation accounts for the excess energy of the thermodynamically unfavorable β phase, which covers an area of $\pi[(r_0 + l_W)^2 - r_0^2]$; $2\pi\sigma(r_0 + l_W)$ is the self-energy of the interface, and the first term represents the loss of configurational entropy involved in preventing the interface from crossing the surface of the substrate [9]. $V(R)$ is of longer range than the relevant van der Waals substrate-interface interaction potential, which is proportional in two dimensions to r_0/R^{p-3} in the limit of $R \ll r_0$, where $p = 6$ and 7 for nonretarded and retarded interactions, respectively [9], and is therefore the only relevant interaction potential in the problem [12]. The case of wetting of a single disk is illustrated in Figs. 2(a) and 2(b), via microconfigurations generated in a computer-simulation calculation on a microscopic interaction model [4].

Under the conditions for wetting of a single disk, bringing two disks close to each other gives rise to two different to-
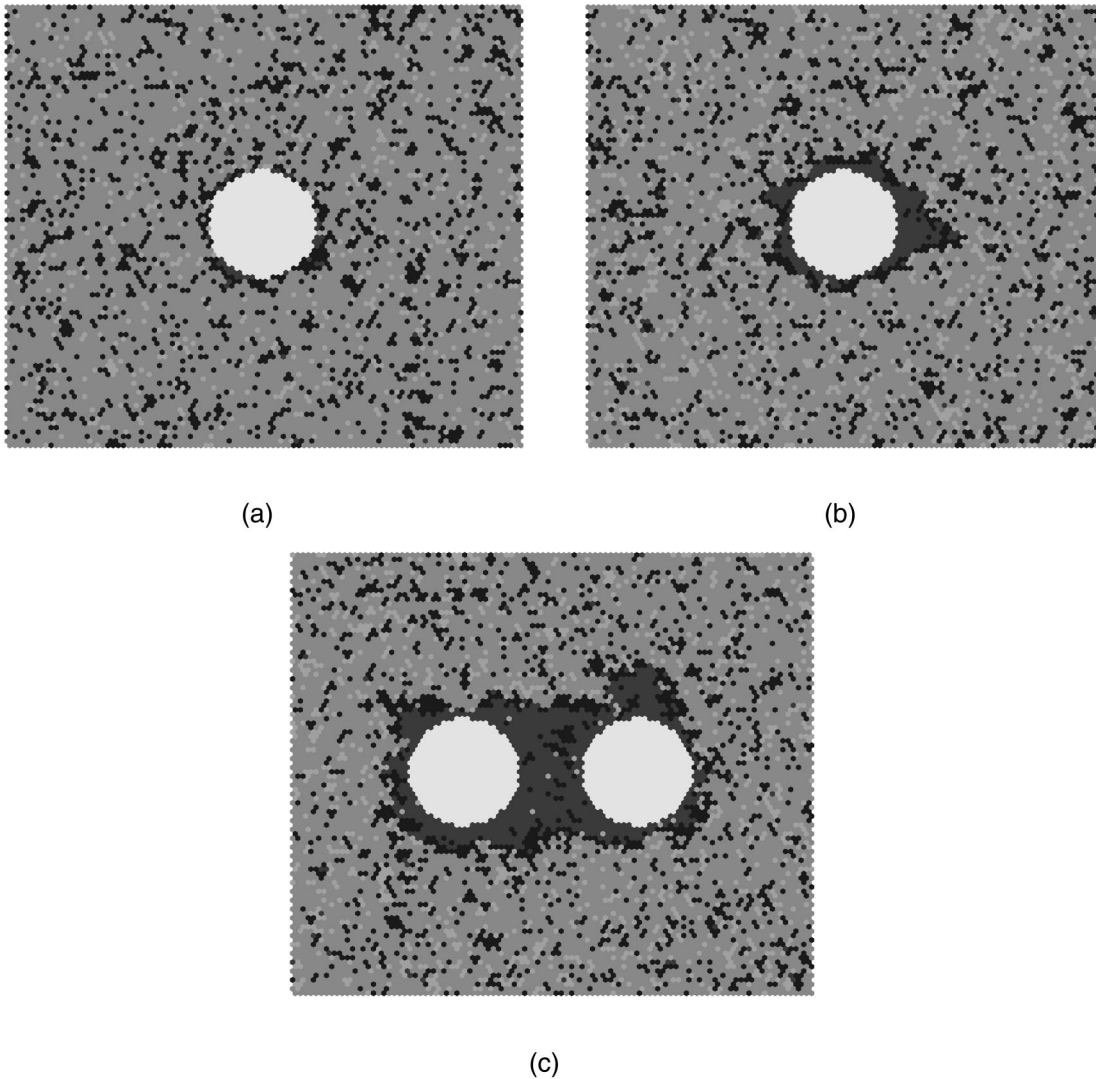
(a)

(b)

(c)

FIG. 2. Illustration of wetting phenomena around circular disks embedded in a binary fluid near an α-β phase transition. The two phases are indicated by light (α) and dark (β) gray tones, respectively. The disks, which have a preference for phase β, are colored white. (a) The case of a single disk outside the wetting regime where only a microscopically thin layer of phase β is present at the interface, corresponding to the case of interfacial adsorption. (b) The case of a single disk in the complete wetting regime. A thick layer of phase β is nucleated at the surface of the disk. (c) The case of two nearby disks in the complete wetting regime, where the wetting layers overlap, leading to capillary condensation. The data for the figures are obtained from computer-simulation calculations on a microscopic model of lipid-protein interactions [4].

pologies of the α-β interface line: one involving two *separate* loops, closing around each one of the disks individually [Fig. 3(a) (sep)]; and one involving a single loop wrapping the two disks [Figs. 3(a) (bri) and 2(c)]. The latter is due to *capillary condensation* between the two disks that occurs to minimize the excess free energy that is associated with a given length of the α-β interface and a given coverage of the thermodynamically unfavorable β phase. A transition between the *separated* and *bridged* configurations can be induced by tuning either the distance between the disks or by changing the thermodynamic conditions for the system, e.g., via Π. Capillary condensation between two wet disks can already take place when the distance between the disks is of the order of their radius r_0. It involves a dramatic increase in the local concentration (or rather the coverage) of the wetting phase β, and introduces a new effective force in the system, giving rise to a net attraction between the disks [11]. The

aggregation force is caused by the tendency of the condensed system to reduce the length of the α-β interface and the coverage of the β phase by reducing the distance between the disks. Capillary-wave fluctuations of the interface were shown not to effect its mean position in the regions where it bridges between the two disks and that, to leading order, the mean position of the remaining interface is given by the theory for the single disk [11].

III. GRAND CANONICAL POTENTIAL
FOR A DILUTE COLLECTION OF DISKS

Now consider a system of N identical ''β-preferring'' mobile disks of radius r_0, immersed in an α fluid. According to the study of capillary condensation between two disks [11], it is reasonable to expect that by tuning the chemical
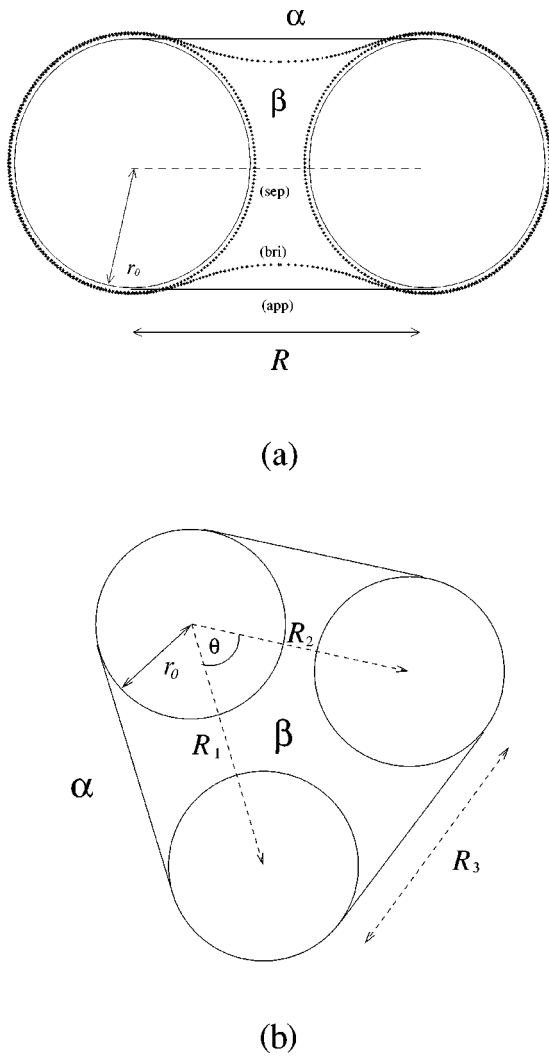
FIG. 3. Illustration of the model interface lines to which a phenomenological interfacial stiffness σ is attached when determining the approximated wetting potential in the case of two and three disks: (a) Two two-dimensional disks of radius r_0 separated at a distance R. The wetting layers surrounding each one of the disks (sep) remain separated until Π is sufficiently small to allow for the formation of a bridging interface (bri) [11]. As an approximation, the bridging interface is taken to be a straight line, tangential to the surfaces of the two disks (app). (b) Three two-dimensional disks of radius r_0 separated at a distances R_1, R_2, and R_3. The interface mean position is approximated by connecting the surfaces of the disks with tangential straight lines.

potential for the fluids close to the α-β transition line (but on the α side) one would reach a region where the disks tend to aggregate and form clusters of disks with a β-rich phase filling the space between them. Within the effective description of the α-β interface [cf. Eq. (5)], we define a cluster as a collection of disks surrounded by the same α-β interface line. When neglecting direct interactions between the disks (apart from the excluded-volume hard disk interactions), the size of those clusters and the cluster-size distribution are controlled by the balance between different entropy effects and the capillary forces which are involved in minimizing the total length of the α-β interface and the coverage of the

β phase. The tendency to increase translational entropy would push the disks apart as well as give rise to a certain cluster-size distribution once clusters are formed. The way the disks (colloids) would arrange themselves inside the clusters is controlled by the interplay between *configurational* entropy, dominating in the colloid fluid phase, and the entropy of *free volume* per disk, dominating in the colloid crystalline phase [13].

We write the *excess* grand canonical potential associated with the creation of clusters in a dilute collection of identical disks in the limit where the interaction among the clusters is negligible. More precisely, we take into account disk-disk interaction potentials only between disks within the same cluster, and neglect direct interactions between disks that belong to different clusters. The sizes of the clusters are parameterized by m, which denotes the number of disks in a cluster. By n_m we denote the number of clusters consisting of m disks, and by $\{n_m\}$ a distribution of cluster sizes. Given a set $\{n_m\}$, we can write the contribution of the *wet* disks to the Hamiltonian of the system as

$$H_{\text{ex}} = \sum_{m=1}^{\infty} \sum_{k=1}^{n_m} \left[W_m(\mathbf{r}_1^{(m,k)}, \ldots, \mathbf{r}_m^{(m,k)}) \right.$$
$$\left. + C_m(\mathbf{r}_1^{(m,k)}, \ldots, \mathbf{r}_m^{(m,k)}) + \sum_{i=1}^{m} \frac{p_{m,k,i}^2}{2c} \right], \quad (6)$$

where $\{n_m\}$ is subject to the restriction $\Sigma_{m=1}^{\infty} m n_m = N$, N being the total number of disks in a given realization of the system. c is the mass of each one of the disks, and $p_{m,k,i}^2/2c$ is the kinetic energy of the ith disk in the kth cluster that consists of m disks. For all clusters of m disks the same $W_m(\mathbf{r}_1, \ldots, \mathbf{r}_m)$ and $C_m(\mathbf{r}_1, \ldots, \mathbf{r}_m)$ functions are defined as an *effective interface potential* and a disk *colloid-colloid* interaction potential, respectively, where $\mathbf{r}_1^{(m,k)}, \ldots, \mathbf{r}_m^{(m,k)}$ are the positions of the m disks that belong to the same cluster. While C_m depends on the positions of the m disks inside the cluster, relative to each other, W_m depends only on the position of the interface surrounding the cluster. A point to which we return later.

With the help of a chemical potential μ_D, which controls the total number of disks in the system, we define and calculate the *excess* factor due to the wet disks in the *grand* partition function of the system as follows:

$$\Xi_{\text{ex}} = \sum_{n_1=0}^{\infty} \sum_{n_2=0}^{\infty} \cdots \sum_{n_m=0}^{\infty} \cdots \frac{1}{n_1! n_2! \cdots n_m! \cdots}$$
$$\times \prod_i \int \frac{d^2 p^i}{h^2} d^2 r^i \{\exp[(\mu_D N - H_{\text{ex}})/k_B T]\}, \quad (7)$$

where h is Plank's constant and $\Lambda = h/(2\pi c k_B T)^{1/2}$ is the thermal (de Broglie) wavelength associated with a disk of mass c. $\Pi_i \int d^2 p^i d^2 r^i$ indicates a multiple integral over all possible values of the components of the momentum $\mathbf{p}_i$ and the position $\mathbf{r}_i$ of every disk for a given cluster-size distribution $\{n_m\}$. Here we have coupled μ_D to the total number of disks, $N = \Sigma_{m=1}^{\infty} m n_m$, for each distribution $\{n_m\}$, and inte-

grated over all possible cluster distributions and thus over all possible values of N. As we neglect interactions between clusters and between disks that belong to different clusters, all clusters of the same size within a given distribution $\{n_m\}$ contribute equally to the trace in Eq. (7). Thus we can write

$$\prod_{i=1}^{N} \int d^2r^i \exp\left\{\sum_{m=1}^{\infty}\sum_{k=1}^{n_m} [W_m(\mathbf{r}_1^{(m,k)},\ldots,\mathbf{r}_m^{(m,k)})+C_m(\mathbf{r}_1^{(m,k)},\ldots,\mathbf{r}_m^{(m,k)})]\right\}$$

$$=\left(\prod_{m=1}^{\infty}\frac{1}{m!}\prod_{i=1}^{m}\int d^2r^i\right)\exp\left\{\sum_{m=1}^{\infty} n_m[W_m(\mathbf{r}_1^{(m)},\ldots,\mathbf{r}_m^{(m)})+C_m(\mathbf{r}_1^{(m)},\ldots,\mathbf{r}_m^{(m)})]\right\}$$

$$=\prod_{m=1}^{\infty}\left(\frac{1}{m!}\prod_{i=1}^{m}\int d^2r^i e^{[W_m(\mathbf{r}_1^{(m)},\ldots,\mathbf{r}_m^{(m)})+C_m(\mathbf{r}_1^{(m)},\ldots,\mathbf{r}_m^{(m)})]}\right)^{n_m}, \tag{8}$$

where $\prod_{i=1}^{m}\int d^2r^i$ indicates a multiple integral over the positions of the m disks belonging to a cluster, and the $1/m!$ factor is to compensate for distinguishing among the disks. Following Eq. (8), we continue with Eq. (7) to obtain

$$\Xi_{\mathrm{ex}}=\prod_{m=1}^{\infty}\sum_{n=0}^{\infty}\frac{1}{n!}\left[e^{m\mu_D/k_BT}\frac{1}{m!}\prod_{i=1}^{m}\int d^2r^i e^{-(C_m+W_m)/k_BT}\prod_{i=1}^{m}\int\frac{d^2p^i}{h^2}e^{-p_i^2/2ck_BT}\right]^n$$

$$=\prod_{m=1}^{\infty}\sum_{n=0}^{\infty}\frac{1}{n!}\left[e^{m\mu_D/k_BT}\Lambda^{-2m}\frac{1}{m!}\prod_{i=1}^{m}\int d^2r^i e^{-(C_m+W_m)/k_BT}\right]^n$$

$$=\exp\left\{\sum_{m=1}^{\infty}\left[e^{m\mu_D/k_BT}\Lambda^{-2m}\frac{1}{m!}\prod_{i=1}^{m}\int d^2r^i e^{-(C_m+W_m)/k_BT}\right]\right\}. \tag{9}$$

Assuming that W_m and C_m depend only on the relative positions of the disks, we rewrite the integral in the last line of Eq. (9) as

$$\Lambda^{-2m}\frac{1}{m!}\prod_{i=1}^{m}\int d^2r^i e^{-(C_m+W_m)/k_BT}$$

$$=\frac{1}{m!}A\Lambda^{-2}\Lambda^{-2(m-1)}\int\cdots\int d\mathbf{r}_1\cdots d\mathbf{r}_{m-1}$$

$$\times e^{-[C_m(\mathbf{r}_1,\ldots,\mathbf{r}_{m-1})+W_m(\mathbf{r}_1,\ldots,\mathbf{r}_{m-1})]/k_BT}$$

$$\equiv A\Lambda^{-2}e^{-V_m/k_BT}, \tag{10}$$

where the $m-1$ vectors $\mathbf{r}_1,\ldots,\mathbf{r}_{m-1}$ describe the relative positions of the m disks. Substituting the definitions of V_m in Eq. (10) into Eq. (9) yields the compact form of

$$\Xi_{\mathrm{ex}}=\exp\left\{A\Lambda^{-2}\sum_{m=1}^{\infty}[e^{(m\mu_D-V_m)/k_BT}]\right\}. \tag{11}$$

The corresponding grand potential $\mathcal{A}_{\mathrm{ex}}$ is readily given by

$$\mathcal{A}_{\mathrm{ex}}=-k_BT\ln\Xi_{\mathrm{ex}}$$

$$=-k_BTA\Lambda^{-2}\sum_{m=1}^{\infty}\exp[(m\mu_D-V_m)/k_BT]. \tag{12}$$

The mean number of disks in the system, $\langle N\rangle$, is the partial derivative of $\mathcal{A}_{\mathrm{ex}}$ with respect to μ_D,

$$\langle N\rangle=A\Lambda^{-2}\sum_{m=1}^{\infty} me^{(m\mu_D-V_m)/k_BT}=\sum_{m=1}^{\infty} m\langle n_m\rangle, \tag{13}$$

where we defined

$$\langle n_m\rangle=A\Lambda^{-2}e^{(m\mu_D-V_m)/k_BT} \tag{14}$$

as the mean number of clusters of size m. For a specific $m=m'$, $\langle n_{m'}\rangle$ can also be obtained by taking the partial derivative $-\partial/\partial(m'\mu_D)$ of $\mathcal{A}_{\mathrm{ex}}$.

To summarize this section, we point out that within the paradigm of an ideal gas of disk clusters, the problem of evaluating the grand canonical potential of the system, $\mathcal{A}_{\mathrm{ex}}$, is reduced in Eq. (12) to the evaluation of the "partition functions" (10) of isolated clusters that consist of m disks. In Sec. IV we study the asymptotic case of $m\gg1$, which is of particular interest since it appears to be the one that determines the conditions at the phase transition between the α-embedded disk cluster-gas phase and the β-embedded disk colloidlike phase (Sec. V). Evaluations of the potentials of small disk clusters will be dealt with in Sec. VI, where we calculate a phase diagram for a particular model of hard disks.

IV. PHENOMENOLOGICAL EFFECTIVE INTERFACE POTENTIAL

Under the assumption that the clusters under consideration are surrounded by a well defined interface line of *stiffness* σ that separates the embedding β phase from the α background phase, the effective potential W_m in Eq. (10) is given by linearly coupling the length of the interface to σ

and the coverage of the β phase to Π, where Π is the *potential difference per unit area* between the β phase and the thermodynamically favorable α phase [11]. Such a W_m can easily be written for any set of $\mathbf{r}_1, \ldots, \mathbf{r}_{m-1}$ vectors, describing the positions of m disks, but the calculations of V_m according to its definition in Eq. (10) becomes very complicated for $m > 3$. However, for very large values of m, we can assume that the clusters minimize the length of interface per unit area by having an underlying geometry of a circle of radius

$$R_m = \sqrt{\frac{m}{\pi \rho_m}}, \qquad (15)$$

where ρ_m is the *number density* of the disks inside a cluster of size m. Then we can approximate the wetting contribution to V_m by replacing r_0 in Eq. (5) with R_m, and by neglecting the contribution coming from the wetting layer which surrounds the whole cluster. Further, we assume that the contribution to V_m coming from the disk-disk interactions within a cluster of size m, i.e., the potential associated with confining m disks within an area of πR_m^2, which we shall denote by V_D, can also be written as a function of ρ_m. Consequently, we obtain an approximate *phenomenological potential*

$$
\begin{aligned}
V_m &= 2\pi R_m \sigma + \pi \Pi (R_m^2 - m r_0^2) + V_D(\rho_m) \\
&= 2\sqrt{\frac{\pi}{\rho_m}} \sigma \sqrt{m} + \Pi\left(\frac{1}{\rho_m} - \pi r_0^2\right) m + V_D(\rho_m) \\
&= \frac{2\pi r_0 \sigma}{\sqrt{\eta_m}} \sqrt{m} + \left[\pi r_0^2 \Pi\left(\frac{1}{\eta_m} - 1\right) + v_D(\eta_m)\right] m, \quad (16)
\end{aligned}
$$

where $\eta_m \equiv \pi r_0^2 \rho_m$ is the volume fraction of the disks inside the cluster and $v_D(\eta_m) \equiv V_D(\eta_m)/m$. The first term in Eq. (16) is the self-energy of a circular interface of radius R_m and stiffness σ. The second term couples the area that is covered by the thermodynamically unfavorable β phase to Π.

The only independent parameter in Eq. (16) is η_m. Thus η_m is defined by minimizing V_D with respect to η_m, i.e., $\partial V_D/\partial \eta_m = 0$, or,

$$
\begin{aligned}
0 &= \frac{\pi r_0 \sigma}{\eta_m^{3/2}} \sqrt{m} + \left(\pi r_0^2 \Pi \frac{1}{\eta_m^2} - \frac{\partial v_D(\eta_m)}{\partial \eta_m}\right) m \Rightarrow \frac{\eta_m^2}{\pi r_0^2} \frac{\partial v_D(\eta_m)}{\partial \eta_m} \\
&= \Pi + \frac{\sigma}{r_0} \sqrt{\frac{\eta_m}{m}} \Rightarrow Z_m(\eta_m) \rho_m k_B T = \Pi + \sigma/R_m, \quad (17)
\end{aligned}
$$

where we have incorporated the fact that $R_m = \sqrt{m/\pi \rho_m} = r_0\sqrt{m/\eta_m}$, and that $Z \equiv \eta(\partial v_D/\partial \eta)/k_B T$ is the *disk compressibility factor*. In the thermodynamic limit, $Z = P/(\rho k_B T)$, where P is the pressure resulting from the colloid disk interactions within a very large aggregate. Hence we can read Eq. (17) as the pressure balance inside a very large cluster, where the expanding pressure due to the disk interaction inside the cluster is balanced by the shrinking pressure due to the chemical potential difference and the Laplace pressure, resulting from the stiffness of the α-β interface.

For further use we now define the dimensionless fields

$$x \equiv r_0 \sigma/k_B T,$$

$$y \equiv r_0^2 \Pi/k_B T, \qquad (18)$$

and remember that we always operate in the limits of $x > 1$ and $y < x$ [cf. Eq. (4)]. With this nomenclature we can rewrite Eq. (16) in the dimensionless form

$$U_m \equiv V_D/k_B T = 2\pi x \sqrt{\frac{m}{\eta_m}} + m\left[\pi y\left(\frac{1}{\eta_m} - 1\right) + f(\eta_m)\right], \qquad (19)$$

where $f \equiv v_D/k_B T$.

Equation (17) implies that in the limit of large enough values of m, η_m is the solution of

$$\eta^2 \frac{\partial f(\eta)}{\partial \eta} = \pi y, \qquad (20)$$

where in this limit $f(\eta)$ can be taken to be the free energy per disk in a pure system of disk colloids. Substituting this solution into Eq. (19) yields that

$$\lim_{m \to \infty} U_m/m = \pi y\left(\frac{1}{\eta'} - 1\right) + f(\eta'), \qquad (21)$$

where η' is the m-independent solution of Eq. (20). Hence we notice that, in the limit of large m, the interfacial term in Eq. (16) is negligible and that U_m/m becomes m independent.

Because V_m [Eq. (19)] grows monotonically with m, the probability to observe large clusters in the system [cf. Eq. (14)] is extremely low. However, as we learn in Sec. V, the properties of the large cluster determine the conditions at the phase transition between the α-embedded disk cluster-gas phase and the β-embedded disk colloidlike phase.

V. TRANSITIONS FROM A CLUSTER GAS OF DISKS TO BULK COLLOIDAL PHASES

The value of the excess free energy $\mathcal{A}_{\text{ex}}$ in Eq. (12) is finite only as long as

$$\lim_{m \to \infty} [V_m - m\mu_D] \geq 0. \qquad (22)$$

Otherwise, $\mathcal{A}_{\text{ex}}$ diverges, indicating an instability of the gas phase and a phase transition. Recalling that for very large values of m, V_m/m reaches an asymptotic m-independent value, we can conclude that this phase transition occurs when the value of $g \equiv \mu_D/k_B T$ approaches [see Eq. (21)]

$$g^* = \lim_{m \to \infty} U_m/m = \pi y\left(\frac{1}{\eta'} - 1\right) + f(\eta'). \qquad (23)$$

Upon increasing the value of g through g^*, the system changes from a phase that consists of finite (small) clusters of disks, of which the size distribution is given by Eq. (14), to a phase that is rich in disks and β fluid, and has the properties of a pure collection of disk colloids. This transi-

tion is first order since the value derivate of $\mathcal{A}$ with respect to μ_D, $\langle N \rangle$, jumps discontinuously as g reaches g^* [see Eq. (24) below].

Noticing that the function $\exp(mg - U_m)$ varies smoothly with g, as long as $g < g^*$, we can calculate the mean disk volume fraction at the transition, $\overline{\eta}^*$, by taking the limit [see Eq. (13)]

$$\overline{\eta}^* = \pi r_0^2 \frac{\langle N \rangle}{A} = \frac{1}{z} \lim_{g \to g^{*-}} \sum_{m=1}^{\infty} m e^{(mg - U_m)}, \qquad (24)$$

where $z \equiv \Lambda^2/(\pi r_0^2)$.

In a system with a fixed disk concentration, $g \to g^{*-}$ leads to a phase separation in which most of the disks aggregate into a large, β-rich domain. In such a system, the chemical potential μ_D depends on the number of disks. In the thermodynamic limit, we can get an idea of this dependence by relating an $\langle N \rangle$-dependent potential, $\Omega_{\text{ex}}(\langle N \rangle)$, to $\mathcal{A}_{\text{ex}}$ in the standard way,

$$\mathcal{A}_{\text{ex}} = \Omega_{\text{ex}}(\langle N \rangle) - \mu_D \langle N \rangle, \qquad (25)$$

where $\langle N \rangle$ is the *expectation* value of the total number of disks in the system given by Eq (13). A corresponding excess free energy per disk, ω_{ex}, is given by [cf. Eqs. (12) and (13)]

$$\omega_{\text{ex}}/k_B T = \frac{\Omega_{\text{ex}}}{\langle N \rangle k_B T} = -\frac{\sum\limits_{m=1}^{\infty} \langle n_m \rangle}{\sum\limits_{m=1}^{\infty} m \langle n_m \rangle} + g. \qquad (26)$$

At the phase separation, where $g = g^*$, both $\Sigma_{m=1}^{\infty} \langle n_m \rangle$ and $\Sigma_{m=1}^{\infty} m \langle n_m \rangle$ diverge, but the ratio between them goes to zero, implying that ω_{ex} becomes approximately g^*, as expected from the low density limit, in which the disks do not contribute to the pressure in the system.

The solution of Eq. (20), substituted into Eq. (23), together with the ability to calculate $\exp(-V_m/k_B T)$ for small values of m [according to Eq. (10)], is what is needed as an input in Eq. (24) when coming to draw a phase diagram that would separate among regions of α-embedded disk cluster-gas and β-embedded bulklike disk systems, and the corresponding coexistence regions. In the following section we study a particular case in which f in Eq. (20) describes a system of hard disks.

VI. THE CASE OF HARD DISKS

In this section we apply the theory that we developed in the previous ones in order to calculate the phase diagram that contains regions of α-embedded disk cluster-gas and β-embedded bulklike disk systems, and the corresponding coexistence regions, in the case of disks that are not allowed to overlap with each other but do not interact otherwise, namely, the so-called hard disks. Hard disk is probably the simplest model of a two-dimensional system of colloids, but it is also the only model for which analytical theories yield a good agreement with computer simulations as concerning the equation of state [6] and the thermodynamic conditions at the

fluid-solid phase transition [7]. Thus we find it suitable for demonstrating the applicability of the theory developed in this paper, yet remaining within an analytical framework. We start by mentioning the theories we applied in calculating the hard disk free energy per disk, f [cf. Eq. (20)], for the fluid and solid phases.

A. Description in the bulk

The questions of whether two-dimensional systems exhibit a ''true'' *fluid-solid* phase transition, and whether this transition is continuous or discontinuous, involving a hexatic intermediate phase or not, are, to different extents, still under debate [14]. Numerous studies, supported by different computer-simulation techniques, have addressed these questions, and it has been shown that a structure factor that is associated with a crystalline order can be measured in large but finite two-dimensional systems. In systems of two-dimensional colloids, the existence of *gas-liquid* and *solid–dense-solid* transitions on top of the *fluid-solid* transition have been shown to depend on the range of the attraction between the colloids [14]. However, in the most simple case of *hard disks*, i.e., disks that are restricted to regions where they do not overlap with each other but do not interact otherwise, only two colloidal phases are observed, *fluid* and *solid*. Extensive computer simulations have so far suggested that the transition between these two phases are first order, without an intervening hexatic phase [15]. Comprehensive theories in which one single expression for the free energy would both account for the fluid and the solid phases of a hard disk system are not found. Instead, separate theories for the fluid and solid phases have been developed, where the special symmetries of the solid phases are taken as an ansatz within a density functional representation of the solid phase [16]. The transition points are then determined by comparing the two free energies and their derivatives, e.g., equating the corresponding pressures and chemical potentials.

In this paper we use an approximate analytical form to describe the excess free energy per hard disk in the fluid phase [6],

$$f_{\text{ex}} = \int_0^{\eta} d\eta' \frac{Z(\eta') - 1}{\eta'}$$

$$= \frac{(2\eta_0 - 1)\ln\left(1 - \frac{2\eta_0 - 1}{\eta_0}\eta\right) - \ln(1 - \eta/\eta_0)}{2(1 - \eta_0)}, \qquad (27)$$

where η is the disk volume fraction and $Z = [1 - 2\eta + (2\eta_0 - 1)\eta^2/\eta_0^2]^{-1}$ is a heuristic hard disk equation of state that exactly reproduces the first two virial coefficients and diverges at the crystalline close-packing volume fraction $\eta_0 = (\sqrt{3}/6)\pi$. In comparison with other analytical approximations, Eq. (27) provides the best combination between simplicity and agreement with results obtained by numerical simulations [6]. f_{ex} is added to the ideal part, $f_{\text{id}} = \ln(\eta z) - 1$, to give the dimensionless free energy per hard disk in the fluid phase, $f_F = f_{\text{ex}} + f_{\text{id}}$. To calculate the free energy of

the hard disk solid phase with the symmetry of a triangular lattice, say f_S, we apply the differential formulation of the GELA [7] with a Percus-Yevick-like approximate equation for the direct correlation function [8],

$$C(d, \eta) = -\Theta(1-d)c_0(\eta)\left[1-4\eta+4\eta w_2\left(\frac{d}{2}\right)+ds_2(\eta)\right],$$ (28)

where $d \equiv R/(2r_0)$, $\Theta(d)$ is the Heaviside step function,

$$w_2(d) = 2\frac{\arccos(d)-d\sqrt{1-d^2}}{\pi},$$ (29)

$$c_0(\eta) = -\frac{1+\eta+3p\eta^2-p\eta^3}{(1-\eta)^3},$$ (30)

and

$$s_2(\eta) = \frac{3}{8}\eta^2\frac{8(1-2p)+(25-9p)p\eta-(7-3p)p\eta^2}{1+\eta+3p\eta^2-p\eta^3}.$$ (31)

$p = \frac{7}{3}-(4\sqrt{3})/\pi$ is related to the approximate hard disk equation of state, $Z_2(\eta) = (1+p\eta^2)/(1-\eta)^2$, which exactly reproduces the first two virial coefficients and is appropriate for use within the GELA that produces low effective liquid densities in the description of the solid phase. As the wetting condition merely alters the pressure of the hard disk system [cf. Eq. (17)], there is nothing to stabilize the square lattice symmetry, and the GELA still predicts a stable two-dimensional solid only on a triangular lattice.

As a check, we calculate the fluid and solid volume fractions at the hard disk fluid-solid transition point by solving for the equilibrium coexistence conditions, $\mu_{\text{fluid}}(\eta_{\text{fluid}}) = \mu_{\text{solid}}(\eta_{\text{solid}})$ and $P_{\text{fluid}}(\eta_{\text{fluid}}) = P_{\text{solid}}(\eta_{\text{solid}})$, where μ is the hard disk chemical potential and P is the pressure. In a very good agreement with the results obtained by a *molecular dynamics* simulation technique ($\eta_{\text{fluid}} = 0.691$, $\eta_{\text{solid}} = 0.716$, $P/(k_BT\rho_{\text{CP}}) = 7.72$) [17] and a *Monte Carlo* simulation technique ($\eta_{\text{fluid}} = 0.690$, $\eta_{\text{solid}} = 0.724$, $P/(k_BT\rho_{\text{CP}}) = 8.08$) [13], we obtain that at the fluid-solid transition point, the corresponding volume fractions are $\eta_{\text{fluid}} = 0.691$, $\eta_{\text{solid}} = 0.724$, and $P/(k_BT\rho_{\text{CP}}) = 7.73$, where ρ_{CP} is the hard disk close-packing density.

B. Wetting controlled phase diagram

Having two hard disk phases, described by the two dimensionless free energies per disk, f_F and f_S, we obtain two solutions to Eq. (20), η'_F and η'_S. Consequently, $\lim_{m\to\infty}U_m/m$ in Eq. (21) takes the lower of the two values, $\pi y(1/\eta'_F-1)+f(\eta'_F)$ and $\pi y(1/\eta'_S-1)+f(\eta'_S)$. Hence, a change in our description of the large cluster occurs at an x-independent value of y, say y_{tr}, that is given by solving numerically the equation set

$$\eta_F^2\frac{\partial f_F(\eta_F)}{\partial \eta_F} = \pi y,$$

$$\eta_S^2\frac{\partial f_S(\eta_S)}{\partial \eta_S} = \pi y,$$ (32)

$$\pi y\left(\frac{1}{\eta_F}-1\right)+f_F(\eta_F) = \pi y\left(\frac{1}{\eta_S}-1\right)+f_S(\eta_S).$$

In the case of hard disks we have obtained that $y_{\text{tr}} = 2.44$, which implies that values of x that are larger than 2.44 [cf. Eq. (18)] are required in order to remain in the complete wetting regime (4) and apply our theory to describe the transition between an α-embedded cluster gas and a β-embedded hard-disk solid.

We are now able to write Eq. (23) for the case of hard disks,

$$g^* = \begin{cases} \pi y\left(\dfrac{1}{\eta_F}-1\right)+f_F(\eta_F), & y<y_{\text{tr}} \\[2ex] \pi y\left(\dfrac{1}{\eta_S}-1\right)+f_S(\eta_S), & y>y_{\text{tr}}, \end{cases}$$ (33)

and learn from Eq. (26) that in the case of phase separation, the hard disk system in the β-rich separated domain can either obtain the characteristics of a colloidal fluid phase (when $y<y_{\text{tr}}$), or the characteristics of a colloidal solid phase (when $y>y_{\text{tr}}$).

To calculate the mean disk volume fraction at the transition, $\bar{\eta}^*$, we should now apply Eq. (24), which requires as an input the $\exp(-U_m)$ functions. In the case of hard disks, the only effect the disk colloid-colloid interaction has is avoiding the disks from overlapping, i.e., the distance between two disks is always larger than their diameter $2r_0$. Then U_m can formally be obtained from [cf. Eq. (10)]

$$e^{-U_m} = \frac{1}{m!}\Lambda^{-2(m-1)}\int_{|\mathbf{r}_1|=2r_0}^{\infty}\cdots\int_{|\mathbf{r}_{m-1}|=2r_0}^{\infty}$$
$$\times d\mathbf{r}_1\cdots d\mathbf{r}_{m-1}e^{-W_m(\mathbf{r}_1,\ldots,\mathbf{r}_{m-1})/k_BT},$$ (34)

where the $m-1$ vectors $\mathbf{r}_1,\ldots,\mathbf{r}_{m-1}$ describe the relative positions of the m disks, and the integrations are carried out under the restriction that for all values of $1 \leq i,j \leq m-1$, $|\mathbf{r}_i-\mathbf{r}_j| > 2r_0$. W_m is the effective interface potential that we here approximate by surrounding a given configuration of m disks by the shortest possible interface. For example, the dimensionless forms of W_1, W_2, and W_3 are (see Fig. 3)

$$W_1/k_BT = 2\pi x,$$ (35)

$$W_2/k_BT = (2\pi+2R/r_0)x+(2R/r_0-\pi)y,$$ (36)

where $R \equiv |\mathbf{r}_1|$ is the distance between the two disks [Fig. 3(a)], and

$$W_3/k_BT=\left[2\pi+\frac{R_1+R_2+R_3}{r_0}\right]x+\left[\frac{\sqrt{(R_1+R_2+R_3)(R_1-R_2+R_3)(R_1+R_2-R_3)(-R_1+R_2+R_3)}}{4r_0^2}\right.$$

$$\left.+\frac{R_1+R_2+R_3}{r_0}-2\pi\right]y,\tag{37}$$

where $R_1\equiv|\mathbf{r}_1|$, $R_2\equiv|\mathbf{r}_2|$, and $R_3=\sqrt{R_1^2+R_2^2-2R_1R_2\cos\theta}$ are the pair distances between the three disks. In the coefficients of x in Eqs. (36) and (37), the first term corresponds to the interface wetting the disks, and the second one to the interface bridging between them. In the coefficient of y in Eq. (36), we subtract the area of a disk from the area of the rectangular defined by the four meeting points of the bridging interface with the disks. In the coefficient of y in Eq. (37), the first term corresponds to the area of the triangle formed by connecting the centers of the disks, the second term corresponds to the complementary area emboarded by the bridging interfaces, and the third (negative) term is the reduction of the area of the disks that was included in the two previous terms.

Substituting Eq. (36) into Eq. (34) yields the result

$$e^{-U_2}=\frac{1}{2!}\Lambda^{-2}2\pi r_0^2\int_2^\infty le^{-[(2\pi+2l)x+(2l-\pi)y]}dl=\frac{(x+y)+1/4}{z(x+y)^2}e^{-[(2\pi+4)x+(4-\pi)y]},\tag{38}$$

where $l\equiv R/r_0$ and $z\equiv\Lambda^2/(\pi r_0^2)$, and substituting Eq. (37) into Eq. (34) yields the integral

$$e^{-U_3}=\frac{1}{3!}\Lambda^{-4}r_0^4\int d\mathbf{l}_1\int d\mathbf{l}_2 e^{-\{[2\pi+l_1+l_2+l_3]x+[\sqrt{(l_1+l_2+l_3)(l_1-l_2+l_3)(l_1+l_2-l_3)(-l_1+l_2+l_3)}/4+l_1+l_2+l_3-2\pi]y\}}$$

$$=2\frac{2\pi}{3!(z\pi)^2}e^{-2\pi(x-y)}\int_2^\infty dl_1\ l_1\int_2^\infty dl_2\ l_2\int_{\theta_{\min}}^\pi d\theta\, e^{-\{[l_1+l_2+l_3]x+[\sqrt{(l_1+l_2+l_3)(l_1-l_2+l_3)(l_1+l_2-l_3)(-l_1+l_2+l_3)}/4+l_1+l_2+l_3]y\}},$$

$$\tag{39}$$

where $\mathbf{l}_i\equiv\mathbf{r}_i/r_0$, $i=1$ and 2, are the scaled position vectors of two disks relative to a third one that is located at the origin, and $\mathbf{l}_3\equiv\mathbf{l}_2-\mathbf{l}_1$. $l_i\equiv|\mathbf{l}_i|=R_i/r_0$, $i=1,2$, and 3, are the dimensionless distances between the disks. θ is the angle between $\mathbf{l}_1$ and $\mathbf{l}_2$ such that $l_3=\sqrt{l_1^2+l_2^2-2l_1l_2\cos\theta}$, and $\theta_{\min}\equiv\arccos[(l_1^2+l_2^2-4)/(2l_1l_2)]$ is the lowest value θ can take for given values of l_1 and l_2 under the hard core condition $l_3\geq2$. The symmetry in the case of three disks allows us to replace the integration over θ from π to 2π by the factor 2, on top of the 2π factor that accounts for the rotational invariance of the system.

Because the integrands in Eqs. (38) and (39) decay exponentially, and vanish at distances much smaller than the mean distances between clusters in the dilute limit, we allow the upper integration limits to reach infinity without affecting the results. Equation (39) can still be integrated numerically for given values of x, y, and z, but, for values of m that are larger than 3, integrating Eq. (34) becomes a formidable task. However, for $g<g^*$, $\exp(mg-U_m)$ is a monotonically descending function and for a certain range of the x, y, and z parameters a good approximation of $\overline{\eta}^*$ can be obtained, cutting the sum in Eq. (24) at $m=3$. The choice of three does of course not apply in general, and the cutoff value of m should be determined according to the required precision for given values of x, y, and z.

In Fig. 4 we plot versus y both $[\Sigma_{m=1}^3 m\exp(mg^*-U_m)]/z$, as an approximation for $\overline{\eta}^*$ [Eq. (24)], and η', the disk volume fraction in the large β-rich domains [see Eq. (21)]. Two values of x are considered, $x=1.2$ and 1.5, and we keep the value of T fixed, in the region where $T_W<T<T_C$ [cf. Eq. (4)], so that in all our calculations $y\propto\Pi$. We have chosen small values of x in order to broaden the cluster-gas region in a phase diagram that would also include high values of $\overline{\eta}$. This allows the full topology of the phase diagram to appear in a single figure. However, it should be noted that for values of y that exceed the given values of x, our theory has to be modified as we leave the complete wetting regime (4) [cf. Eq. (18)]. The main modification would include corrections to the interfacial stiffness associated with thin wetting films at the disk surfaces, but this would not change the topology of the phase diagram. We avoid doing that for the sake of simplicity. The graph (phase diagram) we obtain separates among regions of α-embedded disk cluster-gas and β-embedded hard disk systems, and the corresponding coexistence regions. More specifically, when $\overline{\eta}$, the mean volume fraction of the disks, reaches $\overline{\eta}^*$ from below, the system phase separates and the α-embedded disk cluster gas coexists with a β-embedded colloid phase of hard disks with a local volume fraction η' that is determined by Eq. (21). Upon further increase in $\overline{\eta}$, the pressure in the system remains unchanged and the extent of the β-rich domain grows but without change in the density of the disks inside it, until the point of $\overline{\eta}=\eta'$ is reached and the α fluid becomes metastable in the bulk. For values of $\overline{\eta}$ larger than η', the pressure in the system is no longer dictated by the value of y, but by the equation of state of a β-embedded hard disk sys-
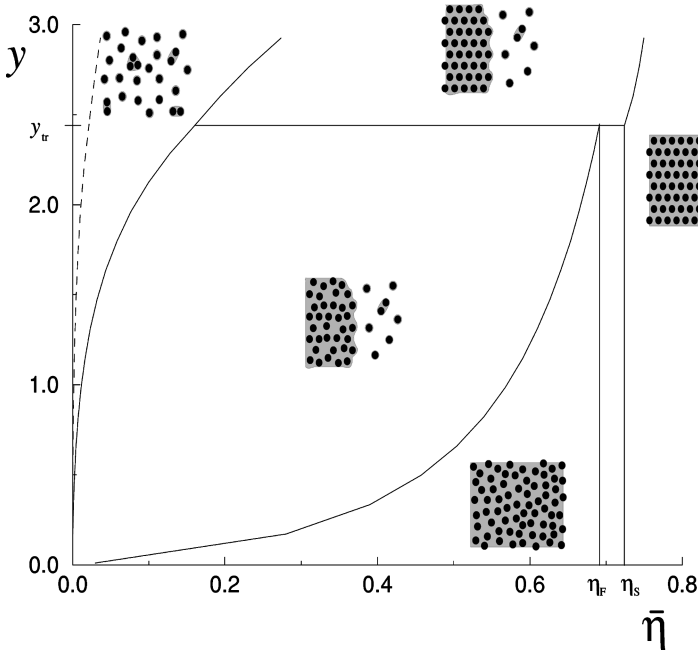
FIG. 4. A calculated phase diagram that contains regions of α-embedded disk cluster gas, β-embedded hard disk liquid, β-embedded hard disk solid, and the corresponding coexistence regions in the ($\bar{\eta}$-y) plane. The different regions are labeled by insets, which are schematic illustrations of the characteristic equilibrium configurations, and in which the white and gray backgrounds represent the α and β phases, respectively. $x=1.2$ and T is kept fixed, $T_W<T<T_C$, so that $y \propto \Pi$. At mean disk-density values for which the α-phase is not stable, the system takes the equilibrium pressure of the corresponding β-embedded hard disk system, independently of the values of y. In the case of $x=1.5$, the condensation line is represented by the dashed line. The horizontal three-phase line extends in this case to connect with the dashed line but the rest of the phase diagram remains unchanged.

tem with a volume fraction $\bar{\eta}$ and a temperature T. Thus, as $\bar{\eta}$ reaches the value of $\eta_{\text{fluid}}=0.691$, a fluid-solid phase separation occurs until $\bar{\eta}$ reaches the value of $\eta_{\text{solid}}=0.724$ and the hard disk system turns solid. In all the relevant calculations $f=f_F$, for $y<y_{\text{tr}}$, and $f=f_S$, for $y>y_{\text{tr}}$. At $y=y_{\text{tr}}$, η' jumps from η'_F to η'_S. These two values are determined by the solution of the equation set (32) and are very close to $\eta_{\text{fluid}}=0.691$ and $\eta_{\text{solid}}=0.724$, which are the corresponding values at the fluid-solid hard disk transition point.

The lower values of $\bar{\eta}$ at which the phase separation occurs, $\bar{\eta}=\bar{\eta}^*$ (Fig. 4), grow with y. The speed of this growth goes down with the increase in the value of x, due to higher values of the interfacial stiffness σ or the radius of the disks r_0.

The justification in taking $m=3$ as a cutoff when $x=1.2$ can be evaluated visually in Fig. 5, where we plot $\exp(g^*-U_1)/\bar{\eta}^*$, $2\exp(2g^*-U_2)/\bar{\eta}^*$, and $3\exp(3g^*-U_3)/\bar{\eta}^*$ as functions y. Up to $y \approx y_{\text{tr}}$, the expectation number of disks that are found as dimers and as trimers grows with y at the expense of the expectation number of monomers. These numbers fall modestly for $y>y_{\text{tr}}$. The reason is that g^* grows faster with y when $y<y_{\text{tr}}$ [cf. Eq. (33)], while $\exp(-U_m)$ descends with y [cf. Eq. (38)]. Under the conditions in which the data shown in Figs. 4 and 5 are calculated, the number of disks that form monomers does not get below 80%. Not more than 25% of the disks are ever expected to form dimers, and not more than 4% to form trimers. Thus neglecting the contribution coming from clusters with more than three disks is a good approximation in the example presented here.

VII. CONCLUSIONS

In general, we have developed an analytical method for calculating the phase diagram of a two-dimensional mixture of disk colloids with two fluid components (α and β), to one of which (β) the disks show a preferential affinity, close to

the fluid-fluid (α-β) first-order phase transition line. In particular, we have calculated an approximate phase diagram for the case of hard disks in the complete wetting regime (4), and observed how the wetting condition adds a gas-liquid transition to a system of hard disks that otherwise show only a fluid-solid transition. This property disappears for $y \geq y_{\text{tr}}$, where $y=\Pi r_0^2/k_B T$, and y_{tr} is the value that corresponds to
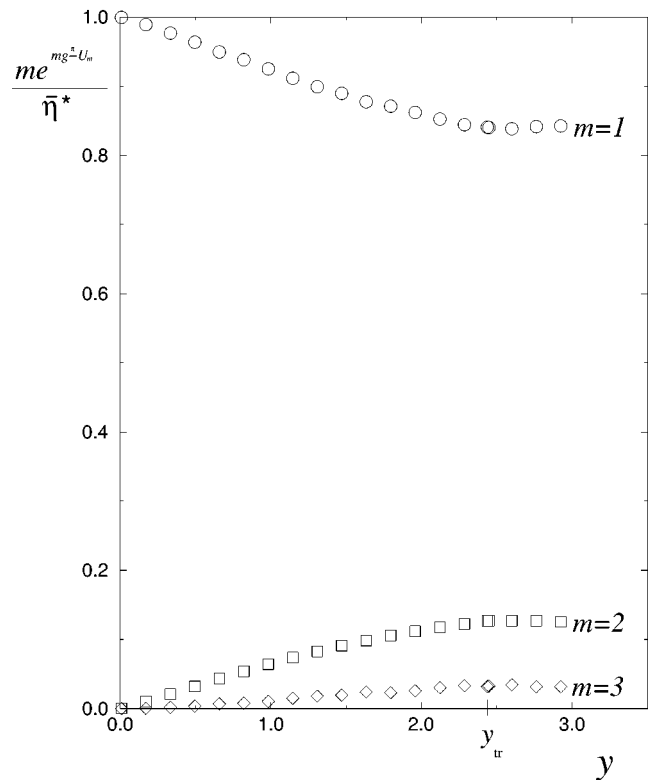

FIG. 5. An estimate of the probability to find a disk in a cluster of size m, $m \exp(mg^*-U_m)/\bar{\eta}^*$, versus y, at the transition value of the disk chemical potential $\mu_D=g^*k_B T$. $x=1.2$, and the temperature is the same as in Fig. 4.

the triple point. Experiments, theory, and computer simulations have shown that the existence of the vapor-liquid transition in systems of colloids depends on the range of the effective colloid-colloid attraction, and that the liquid colloidal phase disappears when the width of the attractive well becomes less than approximately one-third of the diameter of the colloidal spheres [14]. In this sense decreasing y in our model, i.e., approaching the α-β transition conditions, corresponds to increasing the effective range of the pair interactions in systems of interacting disks.

Our method can be applied in three spatial dimensions where a different method [5] has qualitatively predicted a phase diagram that resembles Fig. 4 with two exceptions: one, the earlier studies do not provide a distinction between the different β-rich colloidal phases; two, the prewetting transition line, which distinguishes between regions of wet and non-wet spheres in three dimensions, is not expected in two dimensions [11]. Moreover, the framework developed here enables the calculation of the phase diagram in larger regions of the parameter space than before.

Our theory can be extended to deal with dilute systems of disks outside the complete wetting regime [Eq. (4)]. To do that we need to take into account more configurations of the α-β interface line than the shortest one surrounding the disks in a cluster [cf. Eqs. (35)–(37)] and define two interfacial stiffnesses: one, for the α-β interfaces that bridges between disks, and another one, for the disk-fluid interfaces, outside the complete wetting regime, where the surface of the disks is not wetted by a β-like fluid. However, the qualitative be-

havior observed in this study is not expected to change. In order to include the vicinity of the α-β critical point, the corresponding scaling behavior of the α-β interfacial stiffness σ would have to be included.

In our description of the hard disk colloidal system, we have increased the precision in comparison to previous calculations [7] by applying Eq. (27) for the fluid phase, and simplified the numerical procedures by applying the approximate analytical form of Eq. (28) for the direct correlation function within the GELA.

Our results are relevant under the general interest in the effect the embedding medium can have on the phase behavior of colloids. As a particular case, they can be related to the effect the state of lipids in biological membranes can have on the organization of large inclusions embedded in them, e.g., they can provide a guide for experimentalists to optimize the conditions for protein aggregation and protein crystallization in protein lipid recombinants [4].

[1] Reviews of wetting phenomena can be found, for example, in S. Dietrich, in *Wetting Phenomena* in *Phase Transition and Critical Phenomena*, edited by D. Domb and J. Lebowitz (Academic, New York, 1988), Vol. 12; M. Schick, in *Introduction to Wetting Phenomena*, in *Liquids at Interfaces, Les Houches 1988*, edited by J. Charvolin, J. F. Joanny, and J. Zinn-Justin (North-Holland, Amsterdam, 1990).

[2] D. Beysens and D. Esteve, Phys. Rev. Lett. **54**, 2123 (1985).

[3] Y. Jayalakshmi and E. W. Kaler, Phys. Rev. Lett. **78**, 1379 (1997), and references within.

[4] T. Gil, M. C. Sabra, J. H. Ipsen, and O. G. Mouritsen, Biophys. J. **73**, 1728 (1997).

[5] H. Löwen, Phys. Rev. Lett. **74**, 1028 (1995); Z. Phys. B **97**, 269 (1995).

[6] A. Santos, M. L. de Haro, and S. B. Yuste, J. Chem. Phys. **103**, 4622 (1995).

[7] C. F. Tejero and J. A. Cuesta, Phys. Rev. E **47**, 490 (1993); J. F. Lutsko and M. Baus, Phys. Rev. Lett. **64**, 761 (1990); J. F. Lutsko and M. Baus, Phys. Rev. A **41**, 6647 (1990).

[8] M. S. Ripoll and C. F. Tejero, Mol. Phys. **85**, 423 (1995).

[9] T. Gil and L. V. Mikheev, Phys. Rev. E **52**, 772 (1995).

[10] Close to the bulk α-β critical point T_C, where the bulk correlation length is assumed to be the same in the α and β phases, this definition coincides with the *hyperscaling relation* $\xi_b^{d-1} = \text{const } k_B T / \sigma$, where d is the spatial dimension. However, the theory here is also relevant for temperatures much lower than T_C.

[11] T. Gil and J. H. Ipsen, Phys. Rev. E **55**, 1713 (1997).

[12] R. Lipowsky and M. E. Fisher, Phys. Rev. B **36**, 2126 (1987).

[13] W. G. Hoover and F. H. Ree, J. Chem. Phys. **49**, 3609 (1968).

[14] D. Frenkel, P. Bladon, P. Bolhuis, and M. Hagen, Physica B **228**, 33 (1996), and references within.

[15] J. Lee and K. J. Strandburg, Phys. Rev. B **46**, 11 190 (1992).

[16] R. Evans, in *Density Functionals in the Theory of Nonuniformal Fluids*, in *Fundamentals of Inhomogeneous Fluids*, edited by Douglas Henderson (Dekker, Basel, 1992).

[17] B. J. Alder and T. E. Wainwright, Phys. Rev. **127**, 359 (1962).